Phase transformations of nickeliferous laterites during preheating and reduction with carbon monoxide

Emmanuel N. Zevgolis · Charalabos Zografidis ·
Theodora Perraki · Eamonn Devlin

Abstract This article refers to the mineralogical composition and phase transformations of Greek nickeliferous laterites and to their metallurgical behaviour, during preheating and reduction with carbon monoxide. Transformation of goethite to hematite and decomposition of chlorite and serpentine, were identified during preheating. Higher iron metallization was achieved for the ore in which goethite is the main iron mineral and reduction goes up to 95%, whereas it goes up to 50% for the ore in which hematite is the main iron mineral. The higher reducibility, however, seems to be due to the higher specific surface area of the goethitic type of ore.

Keywords Laterite · Phase transformation · Pyrometallurgy · Reducibility

Introduction

Nickel oxides (laterites) and nickel sulfides comprise the two types of ores used in industrial practice for nickel production. Today, world nickel supply is covered predominantly by sulfide ores (60% against 40% by laterites). Participation of laterite ores, however, has risen from about 10% before 1950 to about 42% in 2003 [1]. And by taking into consideration that any additional nickel demand is expected to be mainly satisfied by mining of laterite deposits, the optimization of the metallurgical laterite processing methods constitutes a great challenge for the nickel industry.

Laterite deposit profiles are classified into the following categories, mainly according to their mineralogical content, [1]: (i) Limonite zone, (ii) Nontronite zone (iii) Serpentine zone and (iv) Garnierite zone. Laterite ores are classified in three classes on the basis of their Fe and MgO content [2]: (i) Class A—garnieritic type of laterites (Fe <12% and MgO >25%). ii) Class B—limonitic type of laterites (high Fe content, 15–32% or >32% and MgO < 10%) and iii) Class C—intermediate type of laterites, that lie between garnieritic and limonitic type of ores (Fe 12–15% and MgO 25–35% or 10–25%).

One of the commonly used processing methods for nickel extraction via pyrometallurgical treatment of lateritic ores includes Electric Furnace (E/F) smelting to ferronickel (Fe-Ni), with a precedent step of preheating and roasting reduction, in Rotary Kiln (R/K) [3]. The target of this work is the mineralogical study of different types of Greek laterite ores, as well as the study of various phase transformations of the ores during preheating and reduction, in order to understand better the extent of their effect on the final reduction obtained.

Greek laterites used for Fe-Ni production, are classified to be of the limonitic type (Class B) and the intermediate type (class C). The main steps involved in the pyrometallurgical treatment of the Greek nickeliferous laterites, the so called 'Larco Process', have already been discussed [4].

E. N. Zevgolis · C. Zografidis (✉) · T. Perraki
School of Mining and Metallurgical Engineering, National
Technical University of Athens, Polytechnioupoli Zografou,
15780 Athens, Greece
e-mail: zografidis@metal.ntua.gr

E. Devlin
NCSR Demokritos, Ag. Paraskevi, 15310 Athens, Greece

Experimental

Characterization of samples

Three different Greek laterite samples were investigated in the present study: Evia island ore (Ore A),

Lokrida ore (Ore B) and Kastoria ore (Ore C), which comprise the main laterite feed of the rotary kilns in the Greek nickel industry. Samples of about 100 kg from each laterite type were collected from the homogenized ore heaps (of approximately 5,000 tons each), ready to be fed to the metallurgical plant. The size analysis of the ores carried out by dry sieving is given in Table 1. It can be seen that the finer fraction (-1 mm) is quite high, ranging from approximately 19 to 27.5%. This constitutes an important operational factor affecting both steps, i.e. roasting and smelting, since it is intimately related with the high amount of dust material in the rotary kilns and also with the lower height of calcine-self-lining, used for protection of Electric Furnace walls from the slag chemical attack.

Chemical analysis of the three bulk ore samples, as well as the ($-12.5 + 9.5$ mm) fraction from each one of the ore samples, which were used for the present reduction experimental study, is given in Table 2. The chemical analysis of the samples was carried out by Atomic Absorption Spectroscopy (AAS), using a Perkin Elmer 2100® instrument. It is deduced that Ores A and B are typical limonitic type (Class B) ores. Ore C is very close to the intermediate type (Class C), given that its chemical analysis does not exactly meet with the requirements of the classification methodology, mentioned previously.

The raw and thermally treated laterites were studied by X-ray diffraction (XRD), Mössbauer spectroscopy and thermo-gravimetric (TG/DTG) and differential thermal analysis (DTA). X-ray powder diffraction patterns were obtained using a Siemens D-5000 diffractometer, with Ni-filtered CuKa radiation ($\lambda = 1.5405$ Å) operating at 40 kV, 30 mA. Differential thermal analysis (DTA) and thermogravimetric analysis (TG/DTG) were obtained simultaneously using a Mettler Toledo 851 instrument. The samples were heated from 20 to 1000 °C at a constant rate of 10 °C min^{-1}.

As revealed from the XRD patterns (Figs. 1 and 2), the samples of Ores A and B mainly consist of hematite (α-Fe_2O_3), as indicated by the characteristic peaks at $d_{104} = 2.69$ Å, $d_{116} = 1.69$ Å, $d_{110} = 2.51$ Å. Quartz ($d_{101} = 3.34$ Å, $d_{100} = 4.26$ Å) and calcite ($d_{104} = 3.03$ Å) are also present in considerable amounts (Figs. 1 and 2). The main Ni-bearing phase is chlorite [(Mg, Ni, Fe, Al)$_6$ (Al, Si)$_4$ O$_{10}$ (OH)$_8$] [5, 6].

In Ore C (Fig. 3) iron is mainly found as goethite (α-FeOOH, $d_{110} = 4.18$ Å, $d_{130} = 2.69$ Å, $d_{111} = 2.45$ Å)

Table 1 Size analysis of the laterite samples

Particle size/mm	Weight/%			Screen opening/mm	Cumulative weight/%		
	Ore A	Ore B	Ore C		Ore A	Ore B	Ore C
+16.0	9.5	8.5	9.8	+16.0	9.5	8.5	9.8
−16 + 12.5	6.2	5.1	3.9	+12.5	15.7	13.6	13.6
−12.5 + 9.5	7.5	4.7	8.9	+9.5	23.3	18.3	22.6
−9.5 + 6.3	10.3	8.9	13.3	+6.3	33.6	27.1	35.8
−6.3 + 3.3	17.1	14.9	18.5	+3.3	50.7	42.1	54.3
−3.3 + 1.7	18.4	17.7	14.3	+1.7	69.1	59.8	687
−1.7 + 1.0	12.1	12.8	8.7	+1.0	81.2	72.6	77.4
−1.0	18.8	27.4	22.6	−1.0			

Table 2 Chemical analysis of the laterite samples (on a dry basis)

Component	Ore A		Ore B		Ore C	
	(Bulk)	(−12.5 + 9.5) mm	(Bulk)	(−12.5 + 9.5) mm	(Bulk)	(−12.5 + 9.5) mm
Fe_2O_3	37.1	37.6	47.7	40.7	26.0	25.2
NiO	1.23	1.12	1.02	0.99	1.5	1.27
SiO_2	32.8	35.8	23.0	31.5	36.7	38.7
CaO	2.9	3.2	2.4	3.7	6.0	4.1
MgO	3.5	3.2	3.0	2.1	11.9	11.4
Al_2O_3	5.2	5.0	10.4	8.0	1.1	1.1
Cr_2O_3	2.6	2.4	2.2	2.0	1.1	1.2
Mn_3O_4	0.3	0.4	0.4	0.3	0.5	0.5
L.O·I.	5.7	5.8	7.8	8.0	15.9	13.2
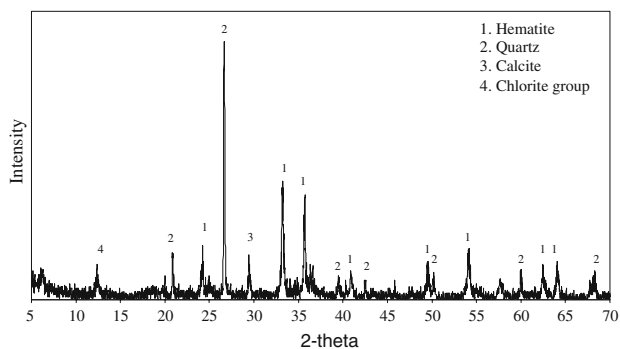
Fig. 1 XRD analysis of Ore A
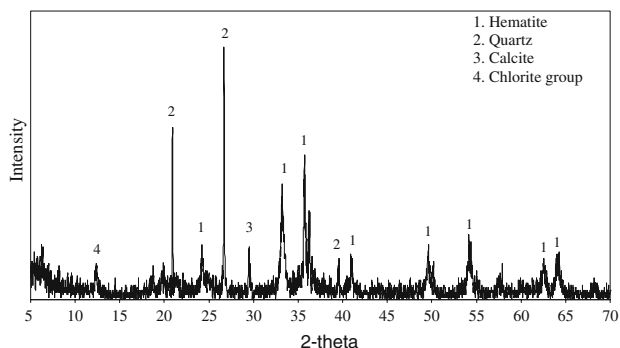
Fig. 2 XRD analysis of Ore B

Fig. 3 XRD analysis of Ore C

Fig. 4 Mössbauer spectra of laterite sample Ore C
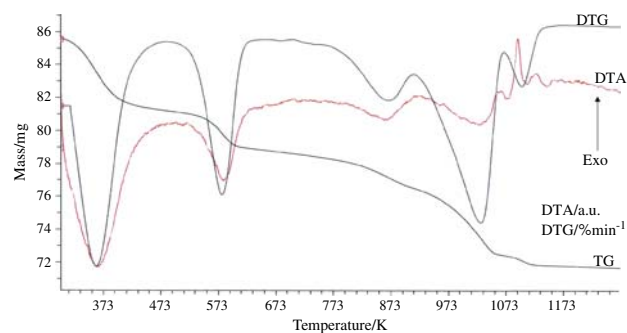
Fig. 5 Thermal analysis of Ore C

Fig. 6 Thermal analysis of Ore B

and the main Ni-bearing mineral phase is serpentine [$(Mg, Fe, Ni)_6Si_4O_{12}(OH)_6$, $d_{101} = 7.3$ Å)].

Mössbauer spectroscopy has been used in the present study for additional quantitative and qualitative appraisal of the iron phases, mainly hematite and goethite, in Ore C. Mössbauer spectra were collected using a conventional transmission spectrometer with a $^{57}Co(Rh)$ source moving with constant acceleration at RT. The relative weights of the iron phases present in these samples are determined from their sub-spectral areas. From the spectra, e.g. Fig. 4, we find that about 80% of the iron content of the sample is present in the form of goethite, 4–5% in the form of hematite and about 13% is ferric iron, which could not be ascribed to any particular certain iron mineral phase.
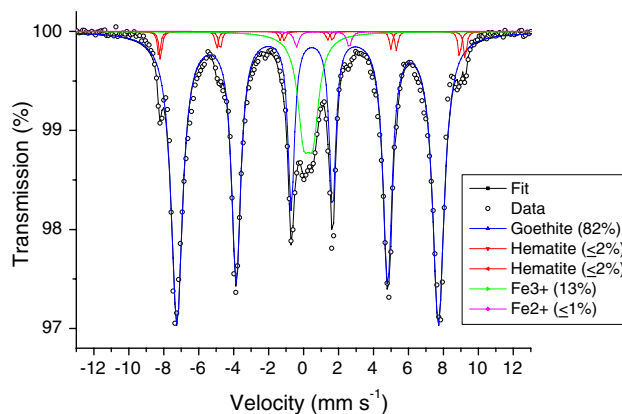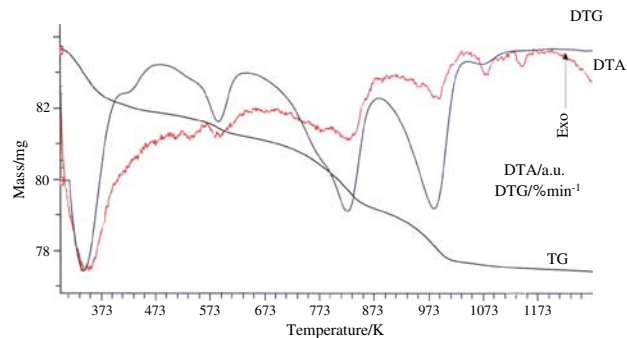
It is noted that hematite in Ore C, although determined by Mössbauer spectroscopy, is not identified by XRD analysis, as seen in Fig. 3. This is attributed to the fact that mineral phases present in such a low content, cannot be determined with X-ray analysis.

TG/DTA diagrams of the pulverized (−200 Mesh) laterite samples, are presented in Figs. 5–7. Four main thermal effects are observed in Fig. 5 (Ore C). The DTG curve of Ore C (Fig. 5) shows four intense peaks at about 100, 300, 600 and 800 °C with a mass loss of 0.6, 2.67, 1.96 and 2.16%, respectively. The first endothermic peak at about 100 °C corresponds to the elimination of water absorbed. The second endothermic peak at about 310 °C corresponds
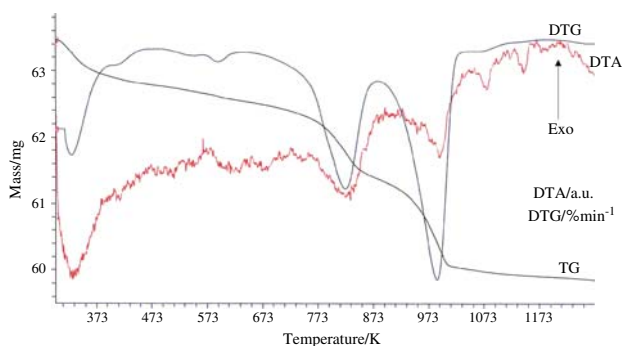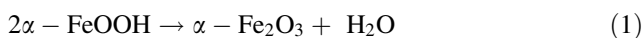
Fig. 7 Thermal analysis of Ore A

to the dehydroxylation of poorly crystallized goethite which is transformed into hematite [7–10] in accordance with Eq. 1.

$$2\alpha - FeOOH \rightarrow \alpha - Fe_2O_3 + H_2O \tag{1}$$

The third endothermic peak at about 600 °C, as well as the exothermic peak at about 830 °C (Fig. 5) represent nickeliferous serpentine [11]. The exothermic peak at 830 °C has been also attributed to recrystallisation phenomena. The fourth endothermic peak at about 780 °C is attributed to calcite decomposition.

Due to the presence of chlorite in Ores A and B an endothermic peak at about 550 °C occurs in DTA diagrams (Figs. 6 and 7). Furthermore, the smaller particle size of calcite in Ores A and B shifts the endothermic peak corresponding to the calcite decomposition to lower temperatures.

The specific surface area of Ores A and C was determined by nitrogen physisorption using a single-point Brunauer–Emmett–Teller (BET) method. Before each measurement the sample was degassed at 250 °C for at least 1 h. It is noted that although the −12.5 + 9.5 mm fraction was used for the conduction of the present preheating and reduction experimental work, the specific surface was determined for the −1.7 + 1 mm fraction of the original sample, due to the limitations of the instrument for the surface are measurement. The specific surface area of Ore A was determined to be 15.52 m^2 g^{-1} while the respective value for Ore C was 82.43 m^2 g^{-1}, that is indicative of the remarkably higher free surface area of the Ore C.

Preheating and roasting reduction

Preheating and reduction experiments of the laterite samples were conducted in an apparatus appropriate for determination of the reducibility of iron ores according to a standard ASTM test method [12]. A thorough description of both the experimental set-up, as well as the preparation of the test samples and the step-by-step conduction of the experiments, has already been discussed [13]. The main steps of the experimental procedure in brief, involved the following: (i) preheating of the test sample (500 g) at a specified size range (−12.5 + 9.5 mm) in a fixed bed at the desired temperature. This includes the steps of heating from 25 °C to the desired temperature at a constant rate of 14 °C/min and calcination at the same temperature under N$_2$ flow, until no further weight loss is recorded for at least 15 min, (ii) isothermal reduction of the test sample at the specified temperature using a reducing gas mixture consisting of CO and N$_2$, (iii) weighing of the test sample at given time intervals and calculation of the state of reduction relative to the ferric iron state, (iv) cooling to room temperature, at a low N$_2$ flow rate.

The experimental procedure of the present study included separate preheating and roasting reduction tests. The scope of preheating tests was to examine the mineral phase transformations that take place, as well as the changes of free surface area of the preheated laterite samples. It is obvious that during preheating, no reduction occurred. Roasting reduction tests were conducted to determine mineral phase transformations during this step and to examine the effect of the mineral and physical properties of the raw laterite samples to the reduction. The degree of reduction after time t, R_t, relative to the ferric iron was calculated according to the requirements of the ASTM standard test method by the following general equation:

$$R_t = (m_t/O_{xh}) \times 100* \tag{2}$$

where m_t is the mass loss, in grams of the test sample after reduction time t.

O_{xh} is the hypothetical oxygen content of test sample at 0% reduction state of the iron and nickel oxides, i.e. assuming that the only iron and nickel oxides present in the laterite sample are Fe$_2$O$_3$ and NiO, respectively. Further mathematical analysis of the parameter O_{xh} has already been discussed [13].

Phase transformations during preheating of the (−12.5 + 9.5) mm fraction

Laterite samples of approximately 500 g each were preheated at specified temperatures, remaining at the desired temperature for 80 min. The criterion for the choice of the 80 min calcination time was that no weight loss was taking place after 80 min, so this was the starting point of the reduction according to the requirements of the ASTM method. Preheating temperatures were taken to be 850 °C for Ores A and B and 400 and 850 °C for Ore C. TG/DTA graphs (Figs. 5–7) indicate that at temperatures above 800 °C, chlorite mineral phase transformation for Ores A and B is taking place and also serpentine transformation for Ore C. Moreover, Ore C was preheated at 400 °C, in order to verify the transformation of goethite. In Figs. 8–10 the
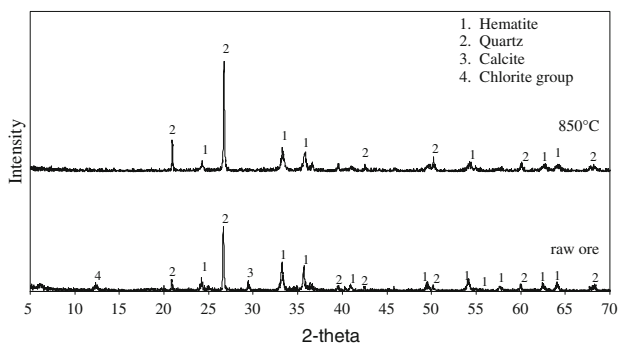
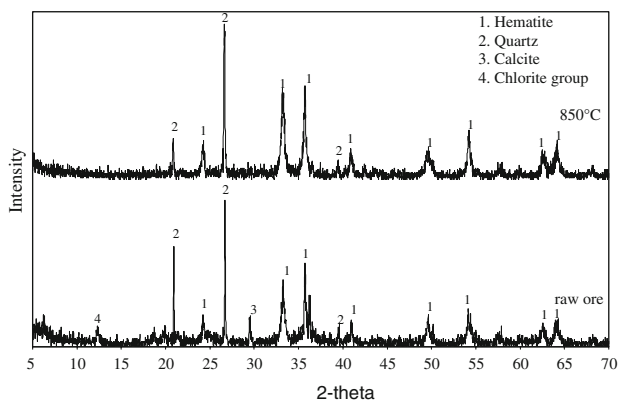**Fig. 8** Mineralogical transformations of Ore A after preheating at 850 °C

Fig. 9 Mineralogical transformations of Ore B after preheating at 850 °C
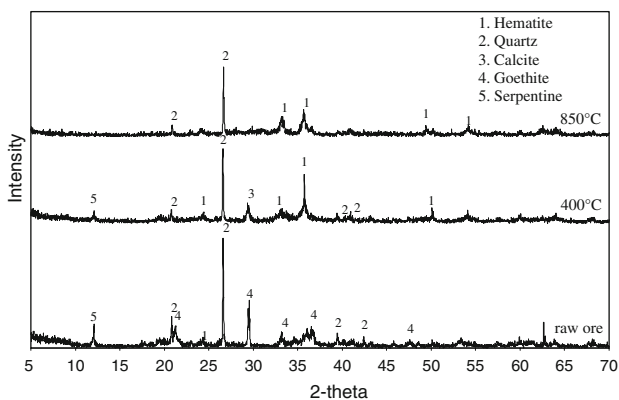

Fig. 10 Mineralogical transformations of Ore C after preheating at 400 and 850 °C

X-ray diagrams of the preheated samples at the specified temperatures are presented.

It is deduced that in the case of hematitic type laterite ores A and B, preheating at 850 °C results in the decomposition of chlorite (Figs. 8 and 9). Additionally, preheating of Ore C at 400 °C results in the transformation of goethite to hematite (Fig. 10). The aforementioned affirms the conclusion deduced by the endothermic peak at about
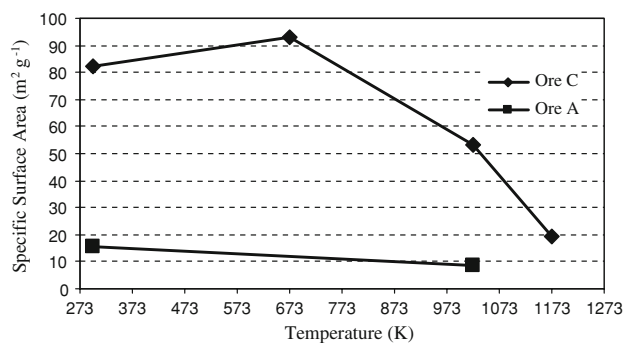

Fig. 11 Effect of temperature of specific surface area of Ores A and C

300 °C on the DTA diagram, which was ascribed to the goethite dehydroxylation. Preheating of Ore C at 850 °C results in the decomposition of serpentine.

The specific surface area determination method of BET was also applied to samples of Ores A and C, calcined for 80 min at 750 °C, in order to examine the effect of preheating on the surface area. The specific area values for Ores A and C were 8.73 and 53.35 m^2/g, respectively, at 750 °C.

Moreover, within the framework of examining the effect of preheating temperature on the surface area of Ore C because of the phase transformation of goethite, its specific surface area was also determined after preheating at 400 and 900 °C. The results are presented in Fig. 11. As it can be seen, dehydroxylation of goethite at temperatures around 400 °C may result in the increase of its specific surface area due to removal of chemically bonded water which may cause the "opening" of the goethite mineral structure. On the contrary, preheating at higher temperatures (750 or 900°C), leads to decrease of specific surface area of both Ores A and C, probably due to coalescence of the narrow pores due to high temperature treatment. The inversely proportional relationship among temperature—within the range 400–900 °C—and specific surface area, comes in agreement with the conclusions deduced by former reducibility studies of iron ores with gaseous reducing agents [14].

Reduction of the (−12.5 + 9.5) mm fraction

In Fig. 12 reduction of the (−12.5 + 9.5) mm fraction, in each of the three laterite samples at temperatures 800, 850 and 900 °C is presented. A detail investigation of reduction as a function of the main reduction parameters such as ore grain size, gas flow rate and others, has been conducted elsewhere [13]. It is apparent from Fig. 12 that reduction progresses with a much higher rate in the case of intermediate type Ore C, than in the case of limonitic Ores A and B. Moreover, reduction degree is around 33 and 38% for Ores A and B, respectively, and 75–92% for Ore C, within the temperature range examined. In the case of Ore

Fig. 12 Reduction degree as a function of time of the $(-12.5 + 9.5)$ mm fractions of: (**a**): Ore A, (**b**): Ore B, (**c**): Ore C, and d) the three laterite samples at 900 °C
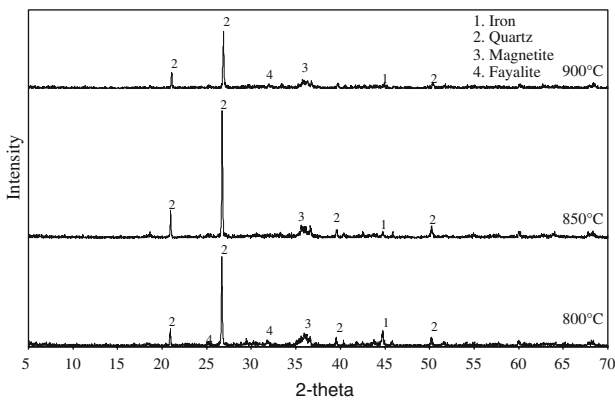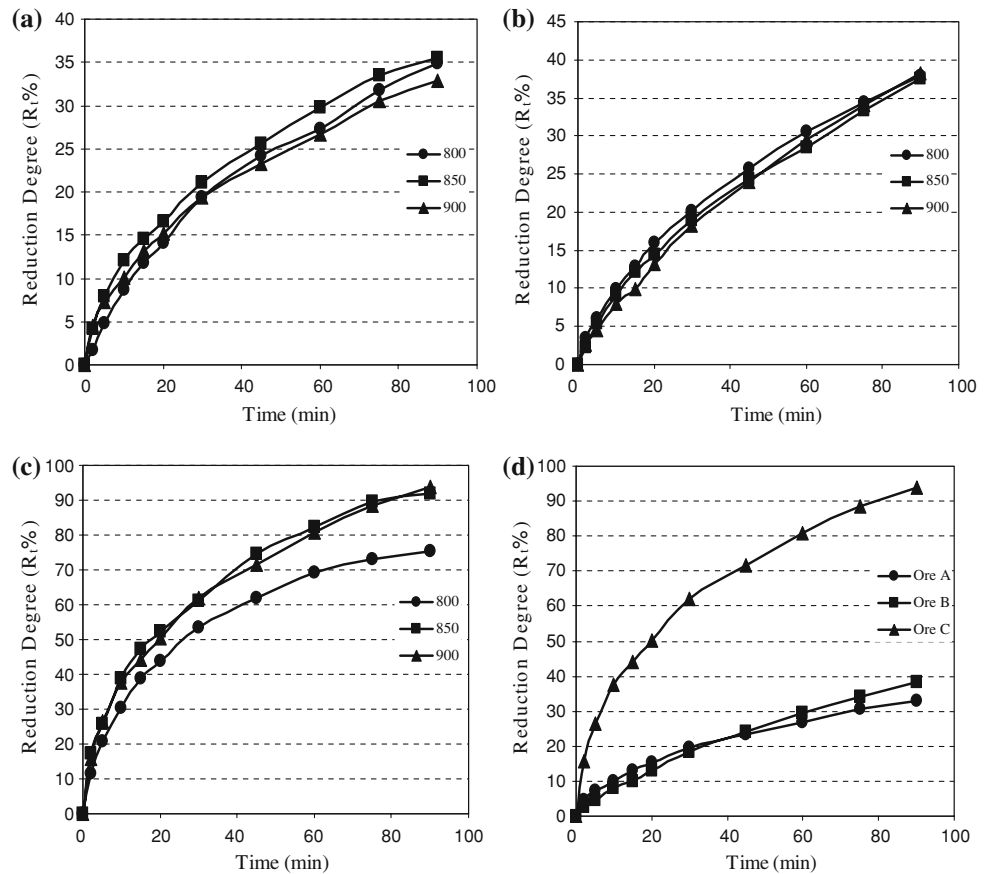

Fig. 13 X-Ray diffraction of Ore A reduced at 800, 850 and 900 °C
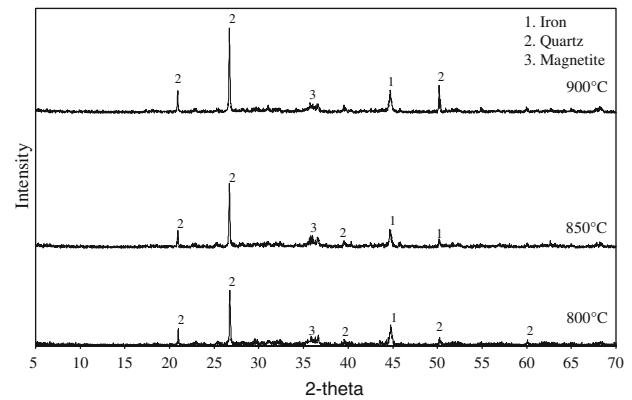

Fig. 14 X-Ray diffraction of Ore C reduced at 800, 850 and 900 °C

C, it can be seen that among 800 and 850 °C there is a noticeable increase in the reduction degree. In all other cases reduction is not affected by temperature within the temperature range examined.

In Figs. 13 and 14, XRD analysis of the reduced samples of Ores A and C, at temperatures 800, 850 and 900 °C is presented. Quartz ($d_{101} = 3.34$ Å, $d_{100} = 4.26$ Å), magnetite (Fe$_3$O$_4$, $d_{311} = 2.53$ Å, $d_{440} = 1.49$ Å) and metallic iron (a-Fe, $d_{110} = 2.03$ Å, $d_{211} = 1.17$ Å), are the mineral phases common in all reduced samples of Ores A

and C. It is also mentioned that calcite does not appear in samples reduced at temperatures higher than 800 °C, due to its thermal decomposition to CaO and CO_2(g) at 850 °C, approximately. As deduced from Fig. 15, where the X-ray diagram of Ores A and C reduced at 850 °C is presented, (based on a qualitative appraisal), metallic iron content is much higher in Ore C than in Ore A. This also holds for the other two temperatures examined. These results, are in agreement with those of chemical analyses of the reduced material from Ores A and C. Apart from the aforementioned
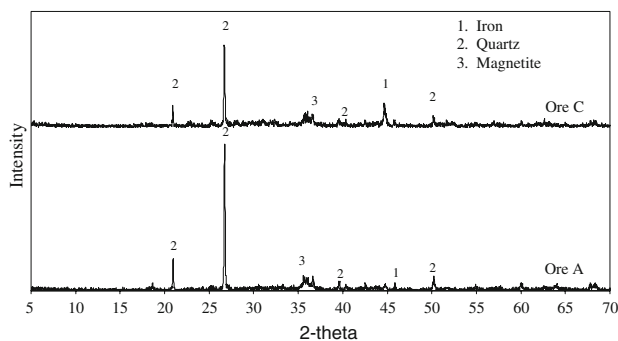
Fig. 15 X-Ray diffraction of Ores A and C reduced at 850 °C

mineral phases, the main mineralogical phase of fayalite ($2FeO.SiO_2$) from the reduced Ore A was detected. Fayalite presence is mainly ascribed to the chlorite thermal decomposition and to the reduction process at the examined temperature range.

Conclusions

This article is focused on the mineralogical composition of the Greek nickeliferous laterites, as well as its effect on the metallurgical behaviour of these ores, during their preheating and reduction with a gaseous reducing mixture ($CO-N_2$).

As it was verified by XRD analysis, Mössbauer spectroscopy and TG/DTA analysis, hematite (Fe_2O_3) is the only iron mineral phase in the limonitic type of the Greek laterites (Ores A and B). Goethite ($a-FeOOH$) is the main iron mineral in the intermediate laterite type. Chlorite [$(Mg, Ni, Fe, Al)_6 (Al, Si)_4 O_{10} (OH)_8$] and serpentine ($Mg, Fe, Ni)_6Si_4O_{12}(OH)_6$, are the main nickel bearing phases regarding limonotic and intermediate type laterites, respectively. Preheating of limonitic type of ore at 850 °C results in chlorite decomposition. Preheating of the intermediate type at 400 °C, results in transformation of goethite to hematite, whereas preheating at 850 °C results in the respective decomposition of serpentine.

Reducibility of intermediate type of Greek laterites is considerably higher than that of the limonitic type under the same experimental conditions. Reduction degree reaches maximum values of approximately 40% for the limonitic type of ore. The respective value for the intermediate type of laterite is 95%. Temperature does not affect reduction within the range of 800–900 °C, for the limonitic type of ore. For the intermediate type of ore, reduction increases when temperature increases from 800 to 850 °C. Specific surface area of intermediate type of laterite is much higher than that of limonitic type and this affects significantly the reducibility of the ore.

Mineralogical analysis of the reduced laterite samples indicated that reduction of ferric to metallic iron is much higher in the intermediate type of laterite ore than in the limonitic type, verifying the results of chemical analyses. Magnetite is also identified in the reduced samples of both types of laterites, and also fayalite ($2FeO \cdot SiO_2$) in the limonitic type of laterites.

References

1. Dalvi AD, Bacon W, Osbourne RC, The past and the future of nickel laterites. In: The Prospectors and Developers Association of Canada (PDAC), editors. Proceedings of the PDAC 2004 International Convention; 2004 March 7–10; Toronto, Canada; 2004. p. 1–27.
2. Zevgolis EN. Extractive metallurgy of nickel: part I. Pyrometallurgical methods. Athens: National Technical University of Athens, editors; 2000 (Greek Text).
3. Zevgolis E, Kontos J. The international picture of nickel metallurgy and the position of the Greek ferronickel industry. In: Proceedings of the 3rd symposium on mineral wealth, Technical Chamber of Greece, Athens, vol A; 2000. p. 107–15 (Greek Text).
4. Zevgolis EN, Zografidis C, Gaitanos J, Kostika I-P, Halikia I. Energy requirements in nickeliferous laterite treatment. In: Howard SM, Stephens RL, Newman CJ, Hwang J-YJ, Gokhale AM, Chen TT, Battle TP, Free ML,. Davis BR, Harris CL, Henein H, Anyalebechi PN, Powell AC, Krumdick GK, Bel CK, editors. Proceedings of the EPD Congress. San Antonio, TX: 2006. p. 487–96
5. Mposkos E, Orfanoudaki A, Perraki Th. The Ni distribution in the mineral phases of Greek Fe-Ni laterite deposits: 2000. In: Proceedings of the 3rd symposium on mineral wealth, Technical Chamber of Greece, Athens, vol A; 2000. p. 107–15 (Greek Text).
6. Albadakis N. Ni-minerals in the deposits of the Sub-Pelagonic zone. Miner Wealth. 1984;31:9–32 (Greek Text).
7. O'Connor F, Cheung WH, Valix M. Reduction roasting of limonite ores: effect of dehydroxylation. Int J Miner Process. 2006;80:88–99.
8. Swamy YV, Kar BB, Mohanty JK. Physico-chemical characterization and sulphatization roasting of low-grade nickeliferous laterites. Hydrometallurgy. 2003;69:89–98.
9. Mackenzie R. Differential thermal analysis, London: Academic Press; 1973.
10. Walter D, Buxbaum G, Laqua WJ. The mechanism of the thermal transformation from goethithe to hematite. J Therm Anal Calorim. 2001;63(3):733–48.
11. Lopez F, Ramirez M, Pons J, Lopez-Delgado A, Alguacil F. Kinetic study of the thermal decomposition of low-grade nickeliferous laterite ores. J Therm Anal Calorim. 2008;94(2):517–22.
12. ASTM standard test method for determination of reducibility of iron ores, Designation: E 1071-85; 1989 (reapproved).
13. Zevgolis EN, Zografidis C, Halikia I, Devlin E. Roasting reduction study of Greek nickeliferous laterites. In: Howard SM, editor. Proceedings of the EPD congress. San Francisco, California; 2009. p. 493–500.
14. Ray HS. Kinetics of metallurgical reactions. New Delhi: Oxford & IBH Publishing Company Pvt. Ltd; 1993.